

This is borne out by the success we had in computing the pressure dependence of the nuclear-quadrupole splitting, which is very sensitive to these low-lying levels. The credibility of the values calculated for the other quantities depends, in addition, on the assumption of a high-spin configuration and the perturbation-theory expressions for these quantities.

We have also investigated the salt KFeF_3 . The value calculated for the cubic splitting $10Dq$ in that salt was determined to be 3900 cm^{-1} . Based upon

our results and the error incurred in the HRH calculation for nickel ion in KNiF_3 , we predict a value of approximately 5500 cm^{-1} for the experimental value of $10Dq$ in KFeF_3 .

ACKNOWLEDGMENTS

The authors would like to thank Professor Martin P. Gouterman for his enlightening comments and the Quantum Chemistry Program Exchange for a copy of the DIATOM program.

*Supported in part by the National Science Foundation and the U. S. Atomic Energy Commission, under Contract No. AT(45-1)-2225.

¹S. Sugano and R. G. Shulman, *Phys. Rev.* **130**, 517 (1963).

²R. E. Watson and A. J. Freeman, *Phys. Rev.* **134**, A1526 (1964).

³D. E. Ellis, A. J. Freeman, and P. Ros, *Phys. Rev.* **176**, 688 (1968).

⁴J. Hubbard, D. E. Rimmer, and F. R. A. Hopgood, *Proc. Roy. Soc. (London)* **88**, 13 (1966).

⁵H. M. Gladney and A. Veillard, *Phys. Rev.* **180**, 385 (1969).

⁶T. F. Soules, J. W. Richardson, and D. M. Vaught, *Phys. Rev. B* **3**, 2186 (1971).

⁷E. Clementi, *IBM J. Res. Develop.* **9**, 2 (1965).

⁸A. C. Switendick and F. J. Corbato, *MIT Solid State Molec. Theory Group Quart. Progr. Rept.* **34**, (1959).

⁹M. P. Barnett and C. A. Coulson, *Phil. Trans. Roy. Soc. London* **A243**, 221 (1951).

¹⁰R. S. Mulliken, *J. Chem. Phys.* **46**, 497 (1947).

¹¹C. W. Christoe and H. G. Drickamer, *Phys. Rev. B* **1**, 1813 (1970).

¹²D. M. Silva, Ph.D. thesis (University of Washington, 1971) (unpublished).

¹³A. Abragam and M. H. L. Pryce, *Proc. Roy. Soc. (London)* **A205**, 135 (1950).

¹⁴D. P. Johnson and R. Ingalls, *Phys. Rev. B* **1**, 1013 (1970).

¹⁵R. Ingalls, *Phys. Rev.* **133**, A787 (1964).

¹⁶A. R. Champion, R. W. Vaughan, and H. G. Drickamer, *J. Chem. Phys.* **47**, 2583 (1967).

¹⁷M. E. Lines, *Phys. Rev.* **156**, 534 (1967).

¹⁸M. E. Lines, *Phys. Rev.* **156**, 543 (1967).

¹⁹R. K. Nesbet, *Ann. Phys. (N. Y.)* **4**, 87 (1958).

²⁰R. K. Nesbet, *Phys. Rev.* **119**, 658 (1960).

²¹H. N. Ok and J. G. Mullen, *Phys. Rev.* **168**, 563 (1968).

²²J. D. Siegwarth, *Phys. Rev.* **155**, 285 (1967).

²³K. Ôno, A. Ito, and T. Fujita, *J. Phys. Soc. Japan* **19**, 2119 (1964).

Estimation of Spectra from Moments—Application to the Hubbard Model*

Michael E. Fisher

Baker Laboratory, Cornell University, Ithaca, New York 14850

and

William J. Camp

Solid State Theory Division-5151, Sandia Laboratories, Albuquerque, New Mexico 87115

(Received 1 November 1971)

We discuss the approximate calculation of a Green's function and its spectral density from its low-order moments by the use of ratio-extrapolation techniques to estimate and factor off the dominant shape of the band edges. The techniques are illustrated, following Brinkman and Rice, on the problem of a single hole propagating in ferromagnetic, antiferromagnetic, and random electron-spin configurations in the atomic limit of the Hubbard model; the methods are, however, of wider applicability.

I. INTRODUCTION

Recently Brinkman and Rice¹ studied the nature of single-particle excitations in the atomic limit of the Hubbard's model² for a magnetic insulator by making use of the sequence of low-order spec-

tral moments. In particular they considered the Green's function, and related spectral density, for a single hole among the N available localized electronic states of a simple-cubic lattice, for which the electronic spins of the $N - 1$ occupied sites were arranged (i) ferromagnetically (F), (ii) antiferromag-

netically (AF), and (iii) randomly (R). Nagaoka³ has shown the ferromagnetic problem to be equivalent to the exactly soluble problem of a single electron in a narrow band. Thus the ferromagnetic single-particle bandwidth is unchanged from that in the spinless case. On the other hand, Brinkman and Rice found significant band narrowing for the random and antiferromagnetic cases: The bands were found to be about 80 and 75%, respectively, as wide as the ferromagnetic band.

This note is a general comment on the extrapolation of the moments in order to estimate the Green's function and spectral density with particular application to the Brinkman-Rice problem. We present improved estimates for the band narrowing which, however, agree quite well with the estimates by Brinkman and Rice. The small differences in bandwidth lead to rather larger differences in the behavior, or "shape," of the Green's function and spectral density near the narrowed-band edge which is described by a "critical exponent." We also address ourselves to the problem of extrapolating the behavior of the spectral density over the whole of the narrowed band. Our method produces a spectral density which (i) is non-negative, (ii) reproduces correctly the known moments, and (iii) incorporates the singular behavior at the band edge. The problem at hand provides an excellent illustration of our general approach.

We shall not reproduce the details of the Hubbard model here or discuss the physics involved. Rather we shall base our discussion directly on the moment series for the spectral density.¹ We forewarn the reader that our approach lacks rigor. Indeed, there exist examples of positive-definite functions which are not uniquely determined by their moments.⁴ Furthermore, there do exist techniques for obtaining exact upper and lower bounds for averages of functions with respect to an unknown spectral density whose first N moments are known.⁵ However, no bounds on the spectral density itself may be obtained from the moments. In practice this may not always be important because the averages over the spectral density, rather than the spectral density, are physically important. However, in many cases the spectrum itself may be observed more or less directly. That our results cannot be correct in detail is seen from the fact that the extrapolation techniques predict a spectral density which goes to zero sharply at the edge of the narrowed band, whereas, as discussed by Brinkman and Rice¹ and by Nagaoka,³ there must be band tails which extend all the way out to the ferromagnetic band edge, although they are probably exponentially damped. We conclude that the apparent singularities found at the narrowed-band edges are probably not real. However, true singularities may appear on the real axis within the band, and it is also

possible that there are pairs of singularities displaced slightly above and below the real axis on the second sheet of the Green's function. In any event we contend that the allowance for singularities, as was partly done by Brinkman and Rice, is essential to a satisfactory simple numerical representation for the spectral density.

The single-hole Green's function $G(\omega)$ and its spectral density $\rho(E) = \rho(-E)$ are related by

$$\omega G(\omega) = \int_{-qt}^{qt} dE \frac{\rho(E)}{1 - (E/\omega)}, \quad (1)$$

with q the lattice coordination number and t the hopping matrix element which enters Hubbard's model.¹ Thus the Taylor-series expansion,

$$\omega G(\omega) = \sum_{l=0}^{\infty} m_{2l} \left(\frac{qt}{\omega}\right)^{2l}, \quad (2)$$

is convergent at least for $|\omega| > qt$, and the coefficients m_{2l} are given by

$$m_{2l} = q^{-2l} M_{2l} = \int_{-qt}^{qt} \left(\frac{E}{qt}\right)^{2l} \rho(E) dE. \quad (3)$$

That is, the m_{2l} are essentially the moments of $\rho(E)$. In Table I we list the first six M_{2l} for the R and AF cases and the first fifteen M_{2l} for the F case, after Brinkman and Rice.¹

II. BAND EDGES AND SHAPES

Rather than directly analyzing $\rho(E)$, we have studied the singular behavior of $G(\omega)$, and using estimates for that, together with the first N exact moments, have formed approximants for $\rho(E)$ over its whole range. We have employed a ratio and Padé-approximant analysis⁶ to study the Green's function. It is convenient to analyze the function $M(\omega)$ defined by

TABLE I. Coefficients M_{2l} (from Brinkman and Rice, Ref. 1).

l	M_{2l} (F)	M_{2l} (AF)	M_{2l} (R)
0		1	1
1		6	6
2		90	72
3		1 860	1 072 $\frac{1}{2}$
4		44 730	17 781 $\frac{3}{4}$
5		1 172 556	314 403
6		32 496 156	
7		936 369 720	
8		27 770 358 330	
9		842 090 474 940	
10		25 989 269 017 140 ^a	
11		813 689 707 488 839 ^a	
12		25 780 447 171 287 800 ^a	
13		625 043 888 527 953 000 ^a	
14		26 630 804 377 937 000 000 ^a	

^aOnly the first 14 figures are accurate.

$$M(w) = \sum_{l=0}^{\infty} m_{2l} w^l. \quad (4)$$

Then we may use the identification $w = (qt/\omega)^2$ to see that

$$C(\omega) = \omega^{-1} M(q^2 t^2 / \omega^2). \quad (5)$$

We estimate the singular point w_c by extrapolating the sequence of ratios

$$\mu_n = m_{2n} / m_{2n-2} \rightarrow w_c^{-1} \text{ as } n \rightarrow \infty \quad (6)$$

vs $(n + \Delta)^{-1}$ for various values of the "n shift," Δ . We choose Δ so as to minimize the curvature of the plot of μ_n vs $(n + \Delta)^{-1}$. It is easily seen that this is a simple method of accounting for the importance of expected higher-order contributions to μ_n varying as n^{-2} . This method has proven very successful in analyzing the nature of singularities at the critical point of the Ising model, for example.⁶ In the presence of sufficiently strong competing singularities on the circle of convergence, the leading corrections will decay less rapidly than n^{-2} and various smoothing devices may be needed. The straightness of the plot can be gauged by comparing estimates of w_c obtained from the intercepts of the straight lines through adjacent pairs of points on the plot with the $n = \infty$ axis. The best values for the singular point ω_c/qt obtained in this manner are found to be 1.000 (F), 0.7405 (AF), and 0.7984 (R), in close agreement with the estimates of Brinkman and Rice, namely, 1.00 (F), 0.742 (AF), and 0.805 (R).¹ Some of the evidence for this is presented in Table II, where we list the successive estimates, $\omega_c(N)/qt$, for N up to 5, obtained by extrapolation through adjacent points for the optimum values of Δ . On using 15 terms in the ferromagnetic series we obtain, with $\Delta = 0.52$, the estimates 0.99998, 0.99999, 1.00000, 1.00001, 1.00001, for $N = 10-14$. From these we estimate $\omega_c/qt = 1 \pm (5 \times 10^{-5})$, which is in excellent accord with the exact result $\omega_c = qt$.

To proceed further we postulate that $M(w)$ may be written as

$$M(w) = B(w) + A(w)[1 - (w/w_c)]^{\nu} \quad (7)$$

for w in the vicinity of w_c , where $A(w)$ and $B(w)$ are analytic, tending to A_c and B_c , as w approaches w_c from below. The "critical" exponent ν may then be estimated by extrapolation of the sequence⁶

TABLE II. Estimates for the singular point from successive pairs of points in the n -shifted ratio plot.

N	(F) $\Delta = 0.56$ $\omega_c(N)/qt$	(AF) $\Delta = 0.89$ $\omega_c(N)/qt$	(R) $\Delta = 0.78$ $\omega_c(N)/qt$
2	0.898	0.7528	0.7937
3	0.988	0.7424	0.7984
4	1.001	0.7405	0.7984
5	1.001	0.7405	0.7984

TABLE III. Estimates for the band-edge exponent ν from successive pairs of points in the n -shifted ratio plot.

N	(F) $\Delta = 0.3$ $\nu(N)$	(AF) $\Delta = 0.9$ $\nu(N)$	(R) $\Delta = 0.8$ $\nu(N)$
2	0.6000	0.2455	0.3425
3	0.5333	0.2652	0.3289
4	0.4935	0.2744	0.3286
5	0.4933	0.2740	0.3284
6	0.4973		
7	0.4982		
8	0.4994		
9	0.4998		
10	0.4999		
11	0.5000		
12	0.5000		
13	0.5000		
14	0.5000		

$$g_n = n[1 - w_c(m_{2n}/m_{2n-2})] \rightarrow 1 + \nu \text{ as } n \rightarrow \infty, \quad (8)$$

vs $(n + \Delta)^{-1}$, again choosing Δ so as to minimize the curvature of the plot of g_n vs $(n + \Delta)^{-1}$.

The relation (8) will be valid even if the amplitude and background functions $A(w)$ and $B(w)$ contain coincident weaker singularities such as $(w_c - w) \ln(w_c - w)$, if $\nu < 1$, but the rate of convergence will in general be slower. Following this procedure we obtain the sequences of estimates for ν shown in Table III. On this basis we estimate for the F case $\nu = 0.500$, which agrees with the rigorous result $\nu = \frac{1}{2}$. Using six moments, however, we could have concluded only that $0.49 \lesssim \nu \lesssim 0.51$. For the AF case we conclude $\nu \approx 0.27$ (which is to be contrasted with Brinkman and Rice's result of 0.195), while for the R case we conclude $\nu \approx 0.33$ (compared with 0.40 as found by Brinkman and Rice). [For the addit of simple fractions we remark that our estimates are not seriously inconsistent with the conjectures $\nu(\text{AF}) = \frac{1}{4}$ and $\nu(\text{R}) = \frac{1}{3}$.]

Since $\nu > 0$, the background constant B_c can be estimated by extrapolation of the sequence of partial sums

$$B_c(N) = \sum_{n=0}^N m_{2n} w_c^n. \quad (9)$$

In this case, however, we must extrapolate $B_c(N)$ vs $(N + \Delta)^{-\nu}$ rather than $(N + \Delta)^{-1}$. To demonstrate this fact, suppose that Eq. (7) holds. Then for large enough n we have, using, say, the binomial theorem and Stirling's theorem,

$$m_{2n} \sim (-)^n \binom{\nu}{n} \sim \frac{1}{n^{\nu+1}}. \quad (10)$$

Hence, as $N \rightarrow \infty$ we find, with b a constant,

$$B_c - B_c(N) \approx b \sum_{n=N}^{\infty} n^{-\nu-1} \approx \left(\frac{b}{\nu}\right) N^{-\nu}, \quad (11)$$

which is the desired result. In this manner we obtain estimates for B_c of 1.515 (F), 3.11 (AF), and 2.42 (R). Brinkman and Rice did not present estimates for the amplitude A_c or background B_c . We may, however, compare our results to those obtained in the Bethe approximation,¹ namely, $A_c = -3.75$, $B_c = 2.50$.

To obtain estimates for A_c , we form the Taylor series of the function $A^*(w)$, given by

$$A^*(w) = [M(w) - B_c] [1 - (w/w_c)]^{-\nu}, \quad (12)$$

and estimate $A_c = A^*(w_c)$. We present the Taylor-series coefficients for $A^*(w)$ in Table IV. Note that they are all negative. We may use two independent techniques to obtain A_c : (i) We form direct Padé approximants⁷ to $A^*(w)$, and evaluate them at w_c ; or (ii) since the series coefficients are all negative, we may use n -shifted ratio techniques to extrapolate the partial sums of $A^*(w_c)$. If $A(w)$ and $B(w)$ in (7) are differentiable near w_c , and $0 < \nu < 1$, then we should extrapolate the partial sums $A_c^*(N)$ vs $(N + \Delta)^{\nu-1}$ because, near w_c ,

$$A^*(w) \approx A_c - w_c B'(w_c) [1 - (w/w_c)]^{1-\nu} - w_c A'(w_c) [1 - (w/w_c)] + \dots, \quad (13)$$

where $A'(w_c)$ and $B'(w_c)$ denote the first derivatives. From the Padé approximants, we obtain, for A_c , -0.68 (F), -2.8 (AF), and -1.9 (R), while from the n -shifted ratios we find -0.71 (F), -2.86 (AF), and -2.00 (R). The Padé-approximant estimates are a few percent lower because they make no allowance for the (weak) singularity of the second term in (13). We thus summarize our analysis of the singular behavior of $G(w)$ by the following three equations:

$$\omega G_F(w) \approx 1.515 - 0.71 [1 - (qt/\omega)^2]^{1/2}, \quad \omega \rightarrow qt + \quad (14a)$$

$$\omega G_R(w) \approx 2.42 - 2.00 [1 - 0.6374(qt/\omega)^2]^{0.33}, \quad \omega \rightarrow 0.7984 qt + \quad (14b)$$

$$\omega G_{AF}(w) \approx 3.11 - 2.86 [1 - 0.5483(qt/\omega)^2]^{0.27}, \quad \omega \rightarrow 0.7405 qt + . \quad (14c)$$

We may obtain an independent check of our estimates for ω_c/qt and ν by using Padé-approximant

TABLE IV. Series coefficients for $A^*(w)$.

n	A_n (F)	A_n (AF)	A_n (R)
0	-0.5000	-2.11000	-1.42000
1	-3.000	-5.37073	-4.68992
2	-45.000	-44.5326	-45.7441
3	-894.000	-498.8133	-598.657
4	-20205.00	-6461.295	-9030.987
5	-490698.0	-91230.51	-148219.36

TABLE V. Polynomial coefficients for the spectral density obtained from N moments without employing $M_c = B_c$. Note that the number of coefficients obtained is equal to the number of moments employed.

n	(F) $N=6$	(F) $N=13$
	p_n	p_n
0	0.86290	0.83861
1	1.2552	3.2179
2	-23.197	-46.709
3	69.695	155.62
4	-81.163	-153.69
5	32.993	-75.592
6		13.051
7		310.49
8		181.55
9		-766.44
10		59.599
11		607.06
12		-288.73

n	(AF) $N=6$
	p_n
0	0.70728
1	0.52950
2	-2.9576
3	10.328
4	-13.912
5	6.2574

n	(R) $N=6$
	p_n
0	0.78562
1	0.06636
2	-3.0543
3	10.130
4	-12.467
5	5.2616

techniques, although six-term series are rather short for this purpose. As a consequence, the convergence of the Padé approximants is not as smooth as that of the ratio extrapolations, so we must be satisfied with, at best, moderate agreement between the methods. Since the singularity in $M(w)$ is weak, we study the function

$$D(w) = \frac{d}{dw} [wM(w)] \approx -\nu A_c \left[1 - \left(\frac{w}{w_c} \right) \right]^{-(1-\nu)} + w_c B'_c + B_c + C_c \left[1 - \left(\frac{w}{w_c} \right) \right]^\nu + \dots \quad (15)$$

From the Padé approximants to $L(w) = (d/dw) \ln D(w)$, we obtain estimates for w_c which are within 0.7% (R), 0.8% (AF), and 2.0% (F) of the ratio estimates. Evaluation of the Padé approximants to the related function $(1 - w/w_c)L(w)$ at $w = w_c$ yields direct estimates for the exponent ν . The estimates for ν are 0.60 (F), 0.28 (AF), and 0.39 (R). In view of the relatively poor convergence of the Padé sequence,

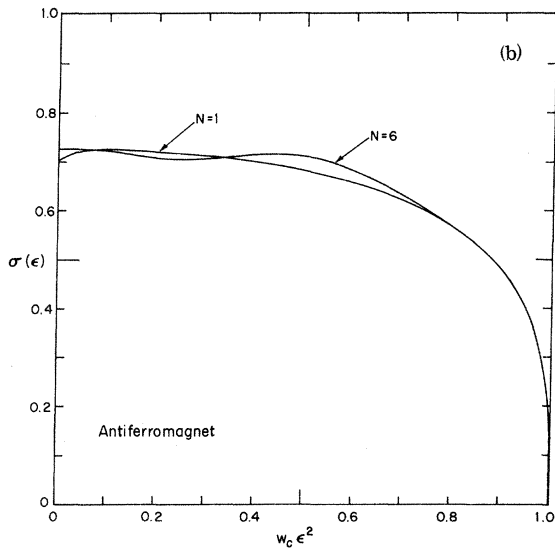
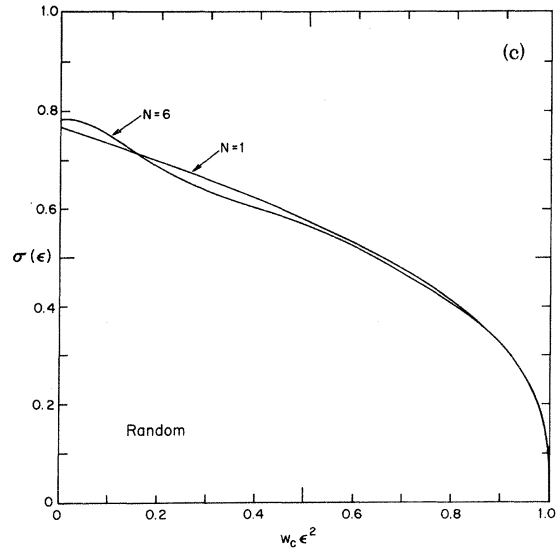
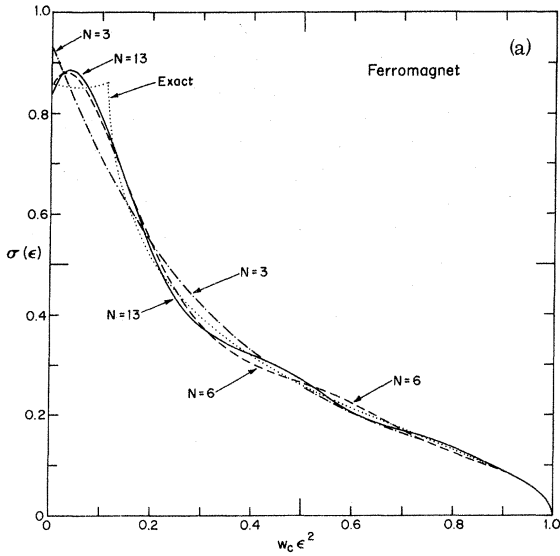


FIG. 1. Reduced spectral densities vs $w_c \epsilon^2$ according to various approximants for the (a) ferromagnetic, (b) antiferromagnetic, and (c) random configurations, with the condition $M_c = B_c$ imposed.

It is easily seen that the form of $M(w)$ postulated in (7) is implied by a function $\sigma(\epsilon)$ of the form

$$\sigma(\epsilon) = R(\epsilon) (1 - w_c \epsilon^2)^\nu, \quad |\epsilon| \leq w_c^{-1/2}$$

$$= 0, \quad |\epsilon| \geq w_c^{-1/2} \quad (18)$$

where $R(\epsilon)$ is an even function, analytic for ϵ near $\pm w_c^{-1/2}$. We will represent $R(\epsilon)$ by the polynomial

$$R(\epsilon) = \sum_{n=0}^{\infty} p_n (\epsilon^2 w_c)^n, \quad (19)$$

and determine coefficients p_n from the Taylor series for $M(w)$. First, note that using (18) and (19), (17) becomes

$$M(w) = \sum_{l=0}^{\infty} \sum_{n=0}^{\infty} w_c^{-1/2} p_n \underline{B}(n+l+\frac{1}{2}, \nu+1) \left(\frac{w}{w_c}\right)^l, \quad (20)$$

where the beta function is, as usual,

$$\underline{B}(x, y) = \int_0^1 du u^{x-1} (1-u)^{y-1} = \frac{\Gamma(x)\Gamma(y)}{\Gamma(x+y)}. \quad (21)$$

Then note that $M_c = M(w_c)$ may be expressed as

$$M_c = B_c = \sum_{n=0}^{\infty} p_n w_c^{-1/2} \sum_{l=0}^{\infty} \underline{B}(n+l+\frac{1}{2}, \nu+1)$$

$$= \sum_{n=0}^{\infty} p_n w_c^{-1/2} \underline{B}(n+\frac{1}{2}, \nu). \quad (22)$$

Comparing (4) with (20) we obtain

$$m_{2l} = w_c^{-1/2-l} \sum_{n=0}^{\infty} p_n \underline{B}(n+l+\frac{1}{2}, \nu+1). \quad (23)$$

Given the first N moments $m_0, m_2, \dots, m_{2N-2}$, and an estimate for M_c , namely, B_c , we can thus

due partly to the residual singularities present in $D(w)$, these are in satisfactory agreement with our ratio results.

III. SPECTRA

We now turn to the task of obtaining $\rho(E)$ from $G(w)$ using (1) and (2). It is convenient to introduce reduced variables

$$\epsilon = (E/qt), \quad \sigma(\epsilon) = qt \rho(qt\epsilon), \quad (16)$$

so

$$\rho(E) = \frac{\sigma(E/qt)}{qt}.$$

Then we have

$$M(w) = \int_{-1}^1 \frac{\sigma(\epsilon) d\epsilon}{1 - \epsilon\sqrt{w}} = \sum_{l=0}^{\infty} w^l \int_{-1}^1 \sigma(\epsilon) \epsilon^{2l} d\epsilon. \quad (17)$$

TABLE VI. Polynomial coefficients for the spectral density obtained from N moments and the value of B_c . Note that $(N+1)$ coefficients are obtained.

n	(F) $N=6$	(F) $N=13$
	p_n	p_n
0	0.848 48	0.837 41
1	2.481 3	3.304 2
2	-39.680	-47.497
3	149.29	155.73
4	-252.50	-136.72
5	201.14	-129.19
6	-61.322	51.139
7		389.77
8		-6.175
9		-596.64
10		74.707
11		338.23
12		4.493 6
13		-101.74

n	(AF) $N=6$
	p_n
0	0.702 19
1	0.948 67
2	-8.432 4
3	36.083
4	-68.059
5	58.260
6	-18.594

n	(R) $N=6$
	p_n
0	0.782 24
1	0.350 59
2	-6.818 9
3	28.033
4	-50.438
5	42.005
6	-13.225

obtain an approximation for $\sigma(\epsilon)$ of the form (18) and (19). The $(N+1)$ coefficients p_n are the components of the vector \vec{p} given by

$$\vec{p} = \underline{K}^{-1} \cdot \vec{m}, \quad (24)$$

where the components of \vec{m} are $m_0, m_2, \dots, m_{2N-2}, M_c = B_c$, and where the elements of the matrix \underline{K} are given by

$$\begin{aligned} K_{l,n} &= w_c^{-l-1/2} \underline{B}(n+l+\frac{1}{2}, \nu+1), \\ & \quad 0 \leq l \leq N-1, \quad 0 \leq n \leq N \\ &= w_c^{-1/2} \underline{B}(n+\frac{1}{2}, \nu), \quad l=N, \quad 0 \leq n \leq N. \end{aligned} \quad (25)$$

If we do not have an estimate for $M_c = B_c$, we can determine the first N coefficients p_0, p_1, \dots, p_{N-1} by using only the components $K_{l,n}$ of \underline{K} with $0 \leq l, n \leq N-1$.

We have generated approximate spectral densities both by employing the condition $M_c = B_c$ and without it. In the former case we can calculate as many as

seven polynomial coefficients from the six-term moment series and in the latter case, up to six coefficients. For the F configuration we have obtained approximations using up to 15 moments, and are able to compare our results with the exact solution. In Table V we list the polynomial coefficients obtained by using six moments for the R and AF configurations and by using six and 13 moments for the F configuration when the condition $M_c = B_c$ was not employed in obtaining the fit. In Table VI we list the polynomial coefficients obtained similarly,

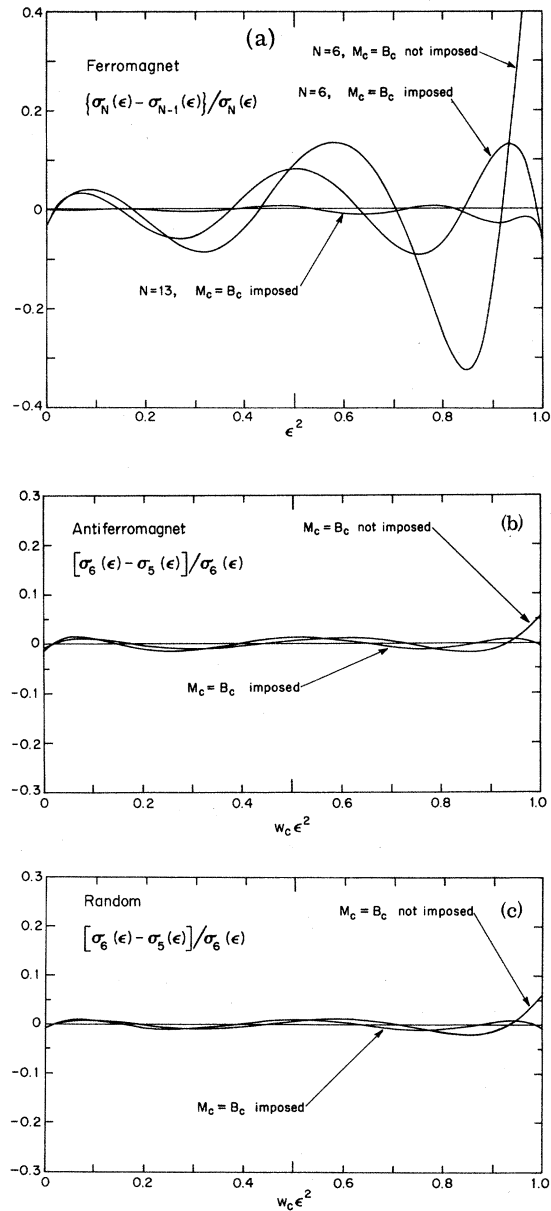


FIG. 2. Measure of the apparent convergence of the spectral approximants for (a) ferromagnetic, (b) anti-ferromagnetic, and (c) random configurations.

but by employing the condition $M_c = B_c$ in the fitting procedure.

The spectral densities obtained from the low-order moments together with B_c are plotted in Fig. 1 using the reduced units introduced in (16). In Fig. 1(a) the approximate spectral densities for the F case obtained by using six and 13 moments are given together with the exact spectral density. In Figs. 1(b) and 1(c) we plot the approximate spectral densities obtained by using one and six moments for the AF and R cases, respectively.

To obtain some measure of convergence of the approximate spectral densities, we plot in Figs. 2(a)–2(c) the normalized difference $[\sigma_6(\epsilon) - \sigma_5(\epsilon)]/\sigma_6(\epsilon)$ between the estimates obtained by using five moments and by using six moments for the three configurations. For the F case we have also included the measure for 12 and 13 moments.

From these figures, we see that (i) the apparent convergence for the R and AF spectral densities (namely, to within 2%) is quite good in comparison to that of the ferromagnetic spectral density (only to within about 10% for $N=6$); (ii) the apparent convergence of the sequence is distinctly better (especially near the band edge) when the condition $M_c = B_c$ is imposed. The relatively poorer convergence of the F sequences is readily understood in the light of the known singular behavior of this spectral den-

sity at low frequencies. The $N=6$ estimate is the first in which representation of this low-frequency singularity is apparent. Thus, it is expected to differ significantly from the $N=5$ estimate, which does *not* show any effects of the singularity. The $N=7$ and $N=8$ estimates already show much better apparent convergence. We could easily have improved our treatment of this case by dividing out the low-frequency singularity as well as that at the band edge. Nevertheless, the approximations obtained above for the ferromagnetic spectral density are perfectly adequate for many purposes, e. g., for estimating the mobility.¹ Finally, we note (iii) that although the fits obtained are slightly oscillatory in character, the spectral densities are found to be everywhere positive. Our best fits to all three spectra are plotted on the same scale in Fig. 3, where we have also indicated the expected small band tails not predicted by the numerical analysis.

In summary, we have shown how to obtain approximations for the spectral density which (i) reproduce correctly all known moments, (ii) contain the appropriate behavior at the leading edge of the band, and (iii) are found to be non-negative. In contrast, Brinkman and Rice used a direct polynomial approximation which gave roughly the correct band narrowing but which did *not* remain positive and did not reproduce the desired behavior near the

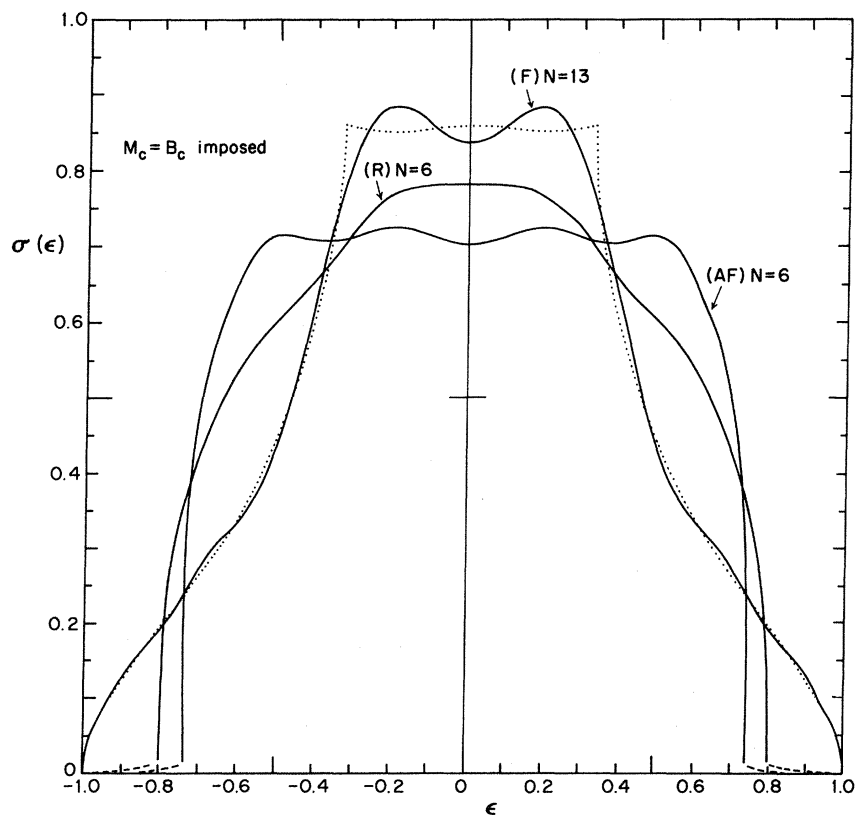


FIG. 3. Best approximants for the reduced spectra vs reduced energy ϵ for all three configurations. The dashed lines represent the expected (but not numerically predicted) band tails. The dotted curve is the exact result for the ferromagnetic case.

band edge. They corrected the first deficiency by fitting the polynomial over the narrowed band, but this approximation also failed to reproduce correctly the behavior near the band edge.

We note that our approach is adaptable to a large variety of situations. For instance, if we also have a Taylor-series expansion for $\rho(E)$, as in the lattice-vibration problem,⁸ we may remove the low-frequency singularity from $\sigma(\epsilon)$ before solving for the polynomial coefficients p_n . While the method certainly does not yield a solution to the so-called moment problem, it does provide a practical technique for obtaining good approximate spectral densities for a large class of Green's functions. Indeed, recent application to exciton line shapes has been made by Doniach, Roulet, and Fisher.⁹ In contrast to the examples considered here, the cor-

responding spectral densities are strongly asymmetric about the origin, and two distinct band-edge exponents must be estimated, but the approach still works well.

ACKNOWLEDGMENTS

We are grateful to Dr. W. F. Brinkman for having brought this problem to our attention and to Dr. B. J. Roulet for comments on a draft manuscript. Some of this work was undertaken while one of the authors (M. E. F.) was holding a John Simon Guggenheim Memorial Fellowship at the Applied Physics Department at Stanford University. The support of the Guggenheim Foundation and the hospitality of Professor Sebastian Doniach are warmly acknowledged.

*Work supported by the U. S. Atomic Energy Commission, by the National Science Foundation, and by the Advanced Research Projects Agency through the Materials Science Center at Cornell University.

¹W. F. Brinkman and T. M. Rice, *Phys. Rev. B* **2**, 1324 (1970).

²J. Hubbard, *Proc. Roy. Soc. (London)* **A276**, 238 (1963); see also Ref. 1 and the references cited therein.

³Y. Nagaoka, *Phys. Rev.* **147**, 392 (1966).

⁴D. V. Widder, *The Laplace Transform* (Princeton U. P., Princeton, N.J., 1946).

⁵J. C. Wheeler and R. G. Gordon, *The Padé Approx-*

mant in Theoretical Physics (Academic, New York, 1970), Chap. 3. This article is a review of the earlier works of Gordon and of Wheeler and Gordon.

⁶M. E. Fisher, *Rept. Progr. Phys.* **30**, 615 (1967); see especially p. 683 and following.

⁷For a discussion of the use of Padé approximants, see Ref. 6.

⁸J. C. Wheeler and R. G. Gordon, *J. Chem. Phys.* **51**, 5566 (1969).

⁹S. Doniach, B. J. Roulet, and M. E. Fisher, *Phys. Rev. Letters* **27**, 262 (1971).

Ferromagnetic Resonance in Ruthenium-Doped Gadolinium Iron Garnet

P. Hansen

Philips Forschungslaboratorium Hamburg GmbH, 2 Hamburg 54, Germany

(Received 30 November 1971)

Ferromagnetic-resonance measurements on single crystals of gadolinium iron garnet doped with ruthenium were carried out at 9.25 GHz in the temperature range 4.2–500 °K. The single-ion model is used to calculate the anisotropy contributions ΔK_1 and ΔK_2 and the field for ferromagnetic resonance. By fitting the theory to the experimental anisotropy data one finds $gH_e = 1.2 \times 10^7$ Oe and $v/\xi = -0.4$, where g , H_e , v , and ξ are the g factor, the exchange field, the one-electron trigonal-field parameter, and the one-electron spin-orbit-coupling parameter, respectively. The linewidth could be interpreted in terms of the longitudinal-relaxation model assigning a short relaxation time of $\tau = 3.3 \times 10^{-12}$ sec to the Ru^{3+} ions.

I. INTRODUCTION

The system $\text{Gd}_3\text{Fe}_{5-x}\text{Ru}_x\text{O}_{12}$ has been studied with respect to the anisotropy and linewidth. A comparison with ruthenium-doped yttrium iron garnet (YIG)^{1,2} is possible, particularly concerning the deduced atomic parameters. Gadolinium iron garnet (GdIG) is also of interest for magneto-optical-storage applications which require a certain magnitude and temperature dependence of the anisotropy field

near the compensation temperature. This can be achieved to a large extent, especially by small dopes with ruthenium.

The contribution of strong anisotropic ions such as Co^{2+} ,^{3,4} Ru^{3+} ,^{1,2,5} and Ir^{4+} to the magnetocrystalline anisotropy could be well explained in terms of the single-ion model.^{6,7} This model requires a sufficient knowledge of the energy levels of these ions and their dependence on the direction of magnetization. For strong anisotropic ions where the